Higher-capacity communication links based on two-mode phase-sensitive amplifiers

C. J. McKinstrie,[1,*] **N. Alic,**[2] **Z. Tong**[3] **and M. Karlsson**[3]

[1]*Bell Laboratories, Alcatel–Lucent, Holmdel, New Jersey 07733*
[2]*Jacobs School of Engineering, University of California at San Diego, La Jolla, California 92093*
[3]*Department of Microtechnology and Nanoscience, Chalmers University of Technology, SE-412 96 Gothenburg, Sweden*
[*]*mckinstrie@alcatel-lucent.com*

Abstract: Optical communication links are usually made with erbium-doped fiber amplifiers, which amplify the signal waves in a phase-insensitive (PI) manner. They can also be made with parametric fiber amplifiers, in which the signal waves interact with idler waves. If information is transmitted using only the signals, parametric amplifiers are PI and their noise figures are comparable to those of erbium amplifiers. However, transmitting correlated information in the signals and idlers, or copying the signals prior to transmission, allows parametric amplifiers to be phase-sensitive (PS), which lowers their noise figures. The information capacities of two-mode PS links exceed those of the corresponding PI links by 2 b/s-Hz.

OCIS codes: (060.2320) fiber optics, amplifiers and oscillators; (190.4380) nonlinear optics, four-wave mixing; (270.2500) fluctuations, relaxation and noise.

References and links

1. R. W. Tkach, "Scaling optical communications for the next decade and beyond," Bell Labs Tech. J. **14** (4), 3–10 (2010).
2. P. J. Winzer, "Modulation and multiplexing in optical communication systems," IEEE LEOS Newsletter **23** (1), 4–10 (2009).
3. P. C. Becker, N. A. Olsson and J. R. Simpson, *Erbium-Doped Fiber Amplifiers* (Academic Press, 1999).
4. M. N. Islam, *Raman Amplifiers for Telecommunications* (Springer Verlag, 2003).
5. J. Hansryd, P. A. Andrekson, M. Westlund, J. Li and P. O. Hedekvist, "Fiber-based optical parametric amplifiers and their applications," IEEE J. Sel. Top. Quantum Electron. **8**, 506–520 (2002).
6. S. Radic and C. J. McKinstrie, "Optical amplification and signal processing in highly-nonlinear optical fiber," IEICE Trans. Electron. **E88C**, 859–869 (2005).
7. C. J. McKinstrie and N. Alic, "Information efficiencies of parametric devices," to appear in IEEE J. Sel. Top. Quantum Electron.
8. R. Loudon, *The Quantum Theory of Light, 3rd Ed.* (Oxford University Press, 2000).
9. J. P. Gordon, W. H. Louisell and L. R. Walker, "Quantum fluctuations and noise in parametric processes II," Phys. Rev. **129**, 481–485 (1963).
10. C. J. McKinstrie and J. P. Gordon, "Field fluctuations produced by parametric processes in fibers," to appear in IEEE J. Sel. Top. Quantum Electron.
11. C. J. McKinstrie, S. Radic and M. G. Raymer, "Quantum noise properties of parametric amplifiers driven by two pump waves," Opt. Express **12**, 5037–5066 (2004).
12. C. J. McKinstrie, M. Yu, M. G. Raymer and S. Radic, "Quantum noise properties of parametric processes," Opt. Express **13**, 4986–5012 (2005).
13. M. Vasilyev, "Distributed phase-sensitive amplification," Opt. Express **13**, 7563–7571 (2005).

#144953 - $15.00 USD
Received 28 Mar 2011; accepted 19 Apr 2011; published 6 Jun 2011

14. C. J. McKinstrie, M. Karlsson and Z. Tong, "Field-quadrature and photon-number correlations produced by parametric processes," Opt. Express. **18**, 19792–19823 (2010).
15. C. E. Shannon, "A mathematical theory of communication," Bell Sys. Tech. J. **28**, 379–423 and 623–656 (1948).
16. T. M. Cover and J. A. Thomas, *Elements of Information Theory, 2nd Ed.* (Wiley, 2006).
17. J. Hansryd and P. A. Andrekson, "Broad-band CW-pumped fiber optical parametric amplifier with 49-dB gain and wavelength-conversion efficiency," IEEE Photon. Technol. Lett. **13**, 194–196 (2001).
18. C. J. McKinstrie and S. Radic, "Phase-sensitive amplification in a fiber," Opt. Express **12**, 4973–4979 (2004).
19. K. Croussore and G. Li, "Phase regeneration of NRZ-DPSK signals based on symmetric-pump phase-sensitive amplification," IEEE Photon. Technol. Lett. **19**, 864–866 (2007).
20. S. Radic, C. J. McKinstrie, A. R. Chraplyvy, G. Raybon, J. C. Centanni, C. G. Jorgensen, K. Brar and C. Headley, "Continuous-wave parametric gain synthesis using nondegenerate-pump four-wave mixing," IEEE Photon. Technol. Lett. **14**, 1406–1408 (2002).
21. R. Tang, J. Lasri, P. S. Devgan, V. S. Grigoryan and P. Kumar, "Gain characteristics of a frequency nondegenerate phase-sensitive fiber-optic parametric amplifier with phase self-stabilized input," Opt. Express **13**, 10483–10493 (2005).
22. J. Kakande, C. Lundström, P. A. Andrekson, Z. Tong, M. Karlsson, P. Petropoulos, F. Parmigiani and D. J. Richardson, "Detailed characterization of a fiber-optic parametric amplifier in phase-sensitive and phase-insensitive operation," Opt. Express **18**, 4130–4137 (2010).
23. E. Desurvire, "Fundamental information-density limits in optically amplified transmission: an entropy analysis," Opt. Lett. **25**, 701–703 (2000).
24. R. Loudon, "Theory of noise accumulation in optical-amplifier chains," IEEE J. Quantum Electron. **21**, 766–773 (1985).
25. Z. Tong, C. J. McKinstrie, C. Lundström, M. Karlsson and P. A. Andrekson, "Noise performance of optical fiber transmission links that use non-degenerate cascaded phase-sensitive amplifiers," Opt. Express **18**, 15426–15439 (2010).
26. Z. Tong, C. Lundström, P. A. Andrekson, C. J. McKinstrie, M. Karlsson, D. J. Blessing, E. Tipsuwannakul, B. J. Puttnam, H. Toda and L. Grüner-Nielsen, "Toward ultra-sensitive optical links enabled by low-noise phase-sensitive amplifiers," to appear in Nat. Photon.
27. J. Tang, "The Shannon capacity of dispersion-free nonlinear optical fiber transmission," J. Lightwave Technol. **19**, 1104–1109 (2001).
28. K. S. Turitsyn, S. A. Derevyanko, I. V. Yurkevich and S. K. Turitsyn, "Information capacity of optical fiber channels with zero average dispersion," Phys. Rev. Lett. **91**, 203901 (2003).
29. R. J. Essiambre, G. J. Foschini, G. Kramer and P. J. Winzer, "Capacity limits of information transport in fiber-optic networks," Phys. Rev. Lett. **101**, 163901 (2008).
30. A. D. Ellis, J. Zhao and D. Cotter, "Approaching the non-linear Shannon limit," J. Lightwave Technol. **28**, 423–433 (2010).

1. Introduction

As network traffic increases, communication systems need to transmit information at higher rates [1]. Not only should such high-capacity systems encode (transmit) information efficiently [2], they should also transport it efficiently. Communication links are sequences of transmission fibers (attenuators), amplifiers (which compensate fiber losses) and detectors. Standard links employ erbium-doped fiber amplifiers [3] or Raman fiber amplifiers [4], which operate on individual signals in phase-insensitive (PI) manners. However, one could also use parametric amplifiers [5, 6], which are based on four-wave mixing (FWM) in fibers. These devices can operate on individual signals or signal–idler (sideband) pairs, in PI or phase-sensitive (PS) manners.

In a previous paper [7], the transmission and detection of information, and the effects on that information of individual attenuators and parametric amplifiers (or frequency convertors), were studied in detail. In this paper, the methods and results of [7] are reviewed briefly, and used to study the information efficiencies of communication links with PI or PS parametric amplifiers. PS amplifiers have lower noise figures (NFs) than PI amplifiers, which (usually) allow PS links to transport information at higher rates than the corresponding PI links.

The analysis of this paper applies to conventional systems with coherent-state (CS) input signals [8], (complex) amplitude-keyed information formats, linear attenuators and amplifiers, and homodyne detectors. For such systems, the signal and idler (sideband) amplitude fluctuations

#144953 - $15.00 USD Received 28 Mar 2011; accepted 19 Apr 2011; published 6 Jun 2011

have Gaussian statistics [9, 10]. This fact has two important consequences. First, the sidebands are specified completely by their amplitude means, variances and correlations. General formulas for the variances and correlations produced by concatenated (multiple-mode) parametric processes are known [11–14]. Second, once the variances and correlations produced by specific links have been determined, the associated information capacities follow from the results of classical information theory [15, 16].

This paper is organized as follows. In Sec. 2, the information capacities of one-mode signals and two-mode signal-idler pairs are defined and discussed briefly. In Sec. 3, the FWM processes that enable PI and PS amplification are reviewed briefly. The noise properties and information capacities of two-mode PI links, one-mode PS links and two-mode PS links are determined in Secs. 4, 5 and 6, respectively, as are the optimal input conditions for these links. Two-mode PS links, which require the inputs to be correlated, have the lowest noise figures and the highest capacities. Finally, in Sec. 7 the main results of this paper are summarized. The measurement of information by homodyne detection was discussed in [7].

2. Input information

The analysis of this paper is based on the assumption that the input signals are CS [8]. For a CS with amplitude mean $\langle a \rangle = \alpha$, where $\langle\ \rangle$ is an expectation value, the quadrature mean $\langle q(\phi) \rangle = (\alpha e^{-i\phi} + \alpha^* e^{i\phi})/2^{1/2}$, where ϕ is the the local-oscillator (LO) phase. $\langle q(0) \rangle$ and $\langle q(\pi/2) \rangle$ are called the real and imaginary quadratures, respectively. Quantum optics theory shows that the quadrature variance $\langle \delta q^2 \rangle = 1/2$, which does not depend on the LO phase, and the associated quadrature distribution has Gaussian statistics. The quadrature fluctuations are called vacuum fluctuations, because they do not depend on the amplitude mean. The quadrature signal-to-noise ratio (SNR) is the square of the quadrature mean divided by the quadrature variance. For a CS and an optimal LO phase, the quadrature SNR is $4|\alpha|^2$.

In the semi-classical model of fluctuations (noise), one replaces the classical signal quadrature x by the semi-classical quadrature $y = x + n$, where n is a Gaussian random variable with mean 0 and (vacuum) variance $\sigma_v = 1/2$. As shown in the Appendix, this ansatz reproduces exactly the quadrature variance of a CS with quadrature mean x.

Let $X = [x_i]^t$ be a vector of signal quadratures and $N = [n_i]^t$ be a vector of noise quadratures with Gaussian statistics. The information content (capacity) of an ensemble (distribution) of signal vectors is maximal if the signal quadratures also have Gaussian statistics [15]. Such distributions are specified completely by their means, variances and correlations. Define the signal covariance matrix $K_x = \langle XX^t \rangle$, the noise covariance matrix $K_n = \langle NN^t \rangle$ and the signal-plus-noise covariance matrix $K_y = K_x + K_n$, and let Δ_n and Δ_y be the determinants of the latter matrices. Then the total information capacity [15]

$$C_t = \ln(\Delta_y/\Delta_n)^{1/2}. \tag{1}$$

The unit of Eq. (1) is nats if the natural logarithm is used, or bits if the base-2 logarithm is used. For each example in this paper, there is only one signal channel, so the capacity (bits) is numerically equal to the spectral efficiency (bits-per-second-per-Hertz) [7]. (This relation does not account for the idler bandwidth.)

For the special case in which there is only one input quadrature, the covariance matrices are scalars and the input capacity

$$C = \ln(1 + \sigma_x/\sigma_v)^{1/2}, \tag{2}$$

where the signal variance (strength) $\sigma_x = \langle x^2 \rangle$ and the noise strength $\sigma_n = \sigma_v$. This capacity depends logarithmically on the ensemble-averaged SNR σ_x/σ_v. Hence, any process that changes the SNR (by changing the numerator or the denominator) also changes the capacity.

#144953 - $15.00 USD Received 28 Mar 2011; accepted 19 Apr 2011; published 6 Jun 2011

For two input quadratures (real and imaginary parts of the same complex amplitude, or quadratures from different amplitudes), the covariance matrices

$$K_y = \begin{bmatrix} \sigma_{11}+\sigma_v & \sigma_{12} \\ \sigma_{12} & \sigma_{22}+\sigma_v \end{bmatrix}, \; K_n = \begin{bmatrix} \sigma_v & 0 \\ 0 & \sigma_v \end{bmatrix}. \tag{3}$$

The first matrix is full, because two input signals can be correlated, whereas the second is diagonal, because the fluctuations associated with orthogonal quadratures of the same CS, or quadratures from independent CS, are uncorrelated. It follows from Eqs. (1) and (3) that the total capacity

$$C_t = \ln[(1+\sigma_{11}/\sigma_v)(1+\sigma_{22}/\sigma_v) - (\sigma_{12}/\sigma_v)^2]^{1/2}, \tag{4}$$

where the signal moments $\sigma_{ij} = \langle x_i x_j \rangle$. The total capacity depends on the individual SNRs and the (normalized) correlation. If the inputs are independent ($\sigma_{12} = 0$), the total capacity is just the sum of the individual capacities. If the total input strength $\sigma_{11} + \sigma_{22}$ is constant, the total capacity decreases as the correlation increases. Hence, any process that changes the correlation also changes the total capacity.

3. Amplification and attenuation

Amplification and attenuation are governed by linear input–output (IO) equations for the operators of the participating modes [11–14]. Quantum optics theory shows that if the input amplitude fluctuations have Gaussian statistics (as they do for CS), so also do the output amplitude fluctuations [9, 10], which are specified completely by their variances and correlations. As shown in the Appendix, the semi-classical model reproduces exactly the output quadrature variances and correlations produced by sequences of parametric processes.

Amplification is made possible by FWM in highly-nonlinear fibers. The modulation interaction (MI) is a degenerate FWM process, in which two pump photons are destroyed, and one signal and one idler photon are created ($2\pi_p \rightarrow \pi_s + \pi_i$, where π_j represents a photon with frequency ω_j) [17]. In the inverse MI, one photon from each of two pumps is destroyed and two signal photons are created ($\pi_p + \pi_q \rightarrow 2\pi_s$) [18, 19]. Both processes are illustrated in Fig. 1. The former process provides two-sideband-mode PS amplification if the signal and idler inputs are nonzero, and two-mode PI amplification if the idler input is zero. The latter process always provides one-mode PS amplification.

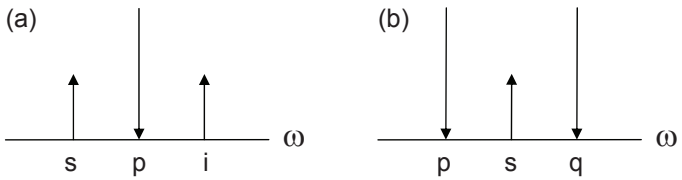

Fig. 1. Frequency diagrams for degenerate four-wave mixing. (*a*) modulation interaction and (*b*) inverse modulation interaction. Downward (upward) arrows denote modes that lose (gain) photons.

Phase conjugation (PC) is a non-degenerate FWM process, in which one photon from each of two pumps is destroyed, and one signal and one idler photon are created ($\pi_p + \pi_q \rightarrow \pi_s + \pi_i$) [20]. This process is illustrated in Fig. 2. It provides two-mode PS amplification if both inputs are nonzero and two-mode PI amplification is one input is nonzero. For both two-mode PS processes, the input idler can be produced by another signal generator, or by a PI amplifier used as a copier prior to transmission [21, 22].

#144953 - $15.00 USD
Received 28 Mar 2011; accepted 19 Apr 2011; published 6 Jun 2011

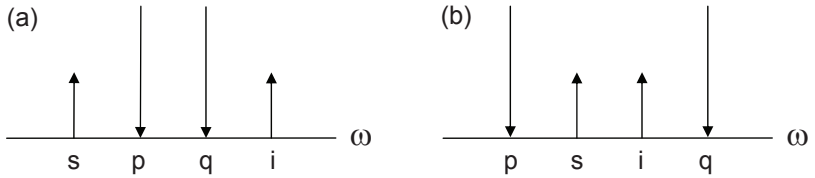

Fig. 2. Frequency diagrams for non-degenerate four-wave mixing. (*a*) outer-band and (*b*) inner-band phase conjugation. Downward (upward) arrows denote modes that lose (gain) photons.

One-mode PS amplification is governed by the IO equations [12, 18]

$$y'_r = (\mu + \nu)y_r, \;\; y'_i = (\mu - \nu)y_i, \tag{5}$$

where y and y' are input and output (signal-plus-noise) quadratures, respectively, and the subscripts r and i denote real (in-phase) and imaginary (out-of-phase) parts, respectively. The transfer coefficients μ and ν (which can be assumed real) satisfy the auxiliary equation $\mu^2 - \nu^2 = 1$, from which it follows that $\mu - \nu = 1/(\mu + \nu)$. The real quadrature is stretched, whereas the imaginary quadrature is squeezed.

Two-mode amplification is governed by the real IO equations [5, 12]

$$y'_{1r} = \mu y_{1r} + \nu y_{2r}, \;\; y'_{2r} = \nu y_{1r} + \mu y_{2r}, \tag{6}$$

where the subscripts 1 and 2 denote the signal and idler modes, respectively. (We used the labels 1 and 2, rather than s and i, because i already denotes imaginary and s will denote stage number.) The imaginary IO equations are similar ($r \to i$ and $\nu \to -\nu$). The signal (information-carrying) contributions to the input quadratures combine coherently, whereas the noise contributions add incoherently. For reference, the real superposition modes $y_\pm = (y_{1r} \pm y_{2r})/2^{1/2}$ obey the IO equations

$$y'_\pm = (\mu \pm \nu)y_\pm, \tag{7}$$

which are equivalent to Eqs. (5). The real sum quadrature ($+$) is stretched, whereas the real difference quadrature ($-$) is squeezed. Similar equations apply to the imaginary superposition quadratures ($\nu \to -\nu$).

Attenuation is modeled as two-mode beam splitting [8, 12], in which signal photons are converted into loss-mode photons ($\pi_s \to \pi_l$). This process is illustrated in Fig. 3. It is governed by the real IO equations

$$y'_{1r} = \tau y_{1r} + \rho y_{lr}, \;\; y'_{lr} = -\rho y_{1r} + \tau y_{lr}, \tag{8}$$

where the subscript l denotes the loss mode, and the transfer coefficients τ and ρ (which also can be assumed real) satisfy the auxiliary equation $\tau^2 + \rho^2 = 1$. The imaginary equations are similar ($r \to i$). The input loss modes are vacuum states.

Equations (5) and (7) show that amplification does not decrease the information capacity by itself, because for each quadrature, the signal and noise components are dilated by the same amount, so the quadrature SNRs are not changed [7]. However, amplification combined with attenuation has a significant effect on capacity. First, consider attenuation followed by amplification. By combining Eqs. (5) or (6) with the first of Eqs. (8), one obtains the composite IO equations

$$y'_\pm = (\mu \pm \nu)\tau y_\pm + (\mu \pm \nu)\rho v_\pm, \tag{9}$$

#144953 - $15.00 USD
Received 28 Mar 2011; accepted 19 Apr 2011; published 6 Jun 2011

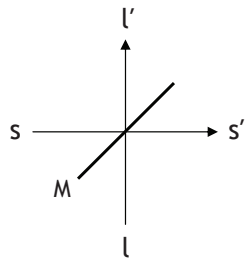

Fig. 3. Illustration of attenuation (modeled as two-mode beam splitting), in which a signal mode (s) interacts with a loss mode (l) at a partially-reflecting mirror (M).

where $v_\pm$ are the loss-mode quadratures (physical or superposition, for one- and two-mode amplification, respectively). Equations (9) show that attenuation reduces the quadrature capacities, by lowering the quadrature SNRs, but subsequent amplification conserves the (reduced) capacities, for the reason stated above. Now consider amplification followed by attenuation, which is governed by the composite IO equations

$$y'_\pm = \tau(\mu \pm \nu)y_\pm + \rho v_\pm. \tag{10}$$

Suppose that $\mu \sim \nu$ and $\mu\tau \sim 1$. Then, for the $+$ mode, the output signal is comparable to the input signal and the attenuator noise is comparable to the transmitted noise. Hence, the output SNR is reduced, but only by a factor of order 1. In contrast, for the $-$ mode, the attenuator noise is much larger than the transmitted noise, and might even be stronger than the transmitted signal, both of which are diminished. Hence, the output SNR is decreased significantly: For all practical purposes, the $-$ mode information is lost. This behavior has important consequences for communication links.

4. Two-mode phase-insensitive links

Two-mode PI links are sequences of attenuators followed by two-mode PI amplifiers, as illustrated in Fig. 4. They are considered first, because of their similarity to standard links, which are based on erbium-doped or Raman fiber amplifiers and are also PI. For the first stage in a two-mode PI link, the (real) IO equations are

$$y_1^{(1)} = (\mu\tau)y_1^{(0)} + (\mu\rho)v_l^{(1)} + \nu v_2^{(1)}, \tag{11}$$

$$y_2^{(1)} = (\nu\tau)y_1^{(0)} + (\nu\rho)v_l^{(1)} + \mu v_2^{(1)}, \tag{12}$$

where $y_1^{(0)}$ is the input signal quadrature, $y_1^{(1)}$ and $y_2^{(1)}$ are the output signal and idler quadratures, respectively, τ and ρ are the transfer coefficients of the attenuator, and μ and ν are the transfer coefficients of the amplifier. The input idler and loss-mode quadratures are denoted by $v_2^{(1)}$ and $v_l^{(1)}$, respectively, to emphasize that these inputs are vacuum states, which originate within the stage. After every stage except the last, the output idler is discarded.

By iterating Eq. (11), one finds that the composite IO equation for an s-stage PI link is

$$y_1^{(s)} = (\mu\tau)^s y_1^{(0)} + \sum_{r=1}^{s} (\mu\tau)^{s-r}[(\mu\rho)v_l^{(r)} + \nu v_2^{(r)}], \tag{13}$$

where $v_2^{(r)}$ and $v_l^{(r)}$ are the idler and loss-mode (noise) quadratures associated with stage r, respectively. For the output idler, only the last stage matters, so

$$y_2^{(s)} = (\nu\tau)y_1^{(s-1)} + (\nu\rho)v_l^{(s)} + \mu v_2^{(s)}. \tag{14}$$

#144953 - $15.00 USD Received 28 Mar 2011; accepted 19 Apr 2011; published 6 Jun 2011

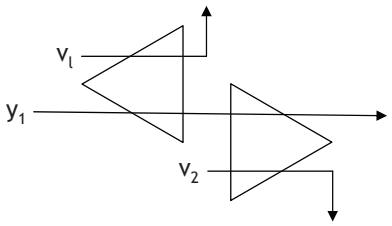

Fig. 4. Architecture of a stage in a two-mode phase-insensitive link. An attenuator ($\triangleleft$) is followed by a two-mode amplifier ($\triangleright$). Modes 1 and 2 are the signal and idler, respectively, and mode l is a loss mode. After every stage except the last, the output idler is discarded.

Define the signal strength $\sigma_x = \langle x_1^2 \rangle$ and the noise strength $\sigma_n = \langle n_1^2 \rangle$. Then the output strengths

$$\sigma_x^{(s)} = (\mu\tau)^{2s}\sigma_x^{(0)}, \tag{15}$$

$$\sigma_n^{(s)} = \{(\mu\tau)^{2s} + [(\mu\rho)^2 + \nu^2][1-(\mu\tau)^{2s}]/[1-(\mu\tau)^2]\}\sigma_v. \tag{16}$$

Equations (15) and (16) are consistent with previous results [12]. On the right side of the latter equation, the first term represents transmitted signal fluctuations, whereas the other terms represent accumulated idler and loss-mode fluctuations.

For a balanced link ($\mu\tau = 1$), the output strengths

$$\sigma_x^{(s)} = \sigma_x^{(0)}, \tag{17}$$

$$\sigma_n^{(s)} = [1 + 2s(L-1)]\sigma_v, \tag{18}$$

where $L = 1/\tau^2$ is the stage loss. The noise figure (NF) of the link is defined to be the input SNR divided by the output SNR. It is a figure of demerit. Because the input and output signal strengths are equal, the NF is just the output noise strength divided by the input (vacuum) strength. Equation (18) shows that the NF increases linearly with the number of stages and the loss of each stage. Notice that amplifier and attenuator noise contribute equally to the link NF.

According to Eq. (1), the output signal capacity

$$C_1^{(s)} = \ln[1 + \sigma_x^{(s)}/\sigma_n^{(s)}]^{1/2}. \tag{19}$$

Compared to the argument of the input logarithm [Eq. (2)], the output argument is reduced by the factor $1 + 2s(L-1) \approx 2sL$, which is the NF of the link. This result is similar to the corresponding result for links with erbium-doped fiber amplifiers [23]. However, parametric links also produce an output idler, which is a copy of the signal, and which also contains information, so the idler and total output capacities should also be determined.

It is instructive to consider the last stage in detail. At the end of stage $s-1$, the signal and noise strengths are $\sigma_x^{(0)}$ and $[1 + 2(s-1)(L-1)]\sigma_v$, respectively. After the last attenuation process, $\sigma_x^{(s-1/2)} = T\sigma_x^{(0)}$ and $\sigma_n^{(s-1/2)} = T[1 + 2(s-1)(L-1)]\sigma_v + (1-T)\sigma_v$, where $T = \tau^2$ is the transmission. At this point, the signal capacity

$$C_1^{(s-1/2)} = \ln[1 + \sigma_x^{(s-1/2)}/\sigma_n^{(s-1/2)}]^{1/2}. \tag{20}$$

Notice that $\sigma_x^{(s-1/2)}/T = \sigma_x^{(s-1)} = \sigma_x^{(s)}$ and $\sigma_n^{(s-1/2)}/T = \sigma_n^{(s-1)} + (L-1)\sigma_v = \sigma_n^{(s)} - (L-1)\sigma_v$. It follows from these results that $C_1^{(s-1)} > C_1^{(s-1/2)} > C_1^{(s)}$. The intermediate capacity is lower than the input (to stage s) capacity because loss-mode fluctuations were added, but is

#144953 - $15.00 USD
Received 28 Mar 2011; accepted 19 Apr 2011; published 6 Jun 2011

higher than the output capacity because idler fluctuations were not (yet) added. Now consider the final amplification process. Equations (6) imply that the output covariance matrices

$$K_y^{(s)} = \begin{bmatrix} \mu^2(\sigma_x+\sigma_n)+\nu^2\sigma_v & \mu\nu(\sigma_x+\sigma_n+\sigma_v) \\ \mu\nu(\sigma_x+\sigma_n+\sigma_v) & \nu^2(\sigma_x+\sigma_n)+\mu^2\sigma_v \end{bmatrix}, \quad (21)$$

$$K_n^{(s)} = \begin{bmatrix} \mu^2\sigma_n+\nu^2\sigma_v & \mu\nu(\sigma_n+\sigma_v) \\ \mu\nu(\sigma_n+\sigma_v) & \nu^2\sigma_n+\mu^2\sigma_v \end{bmatrix}, \quad (22)$$

where the superscripts $s-1/2$ on σ_x and σ_n were omitted for brevity. It is easy to verify that the determinant $\Delta_n = \sigma_n\sigma_v$ and, hence, that $\Delta_y = (\sigma_x+\sigma_n)\sigma_v$. It follows from these results and Eq. (1) that the output idler capacity

$$\begin{aligned} C_2^{(s)} &= \ln\{1+\sigma_x^{(s-1/2)}/[\sigma_n^{(s-1/2)}+L\sigma_v/(L-1)]\}^{1/2} \\ &= \ln\{1+\sigma_x^{(s)}/[\sigma_n^{(s)}+(2L-1)\sigma_v/(L-1)]\}^{1/2}, \end{aligned} \quad (23)$$

where the superscripts were restored for clarity. In the high-loss regime ($L \gg 1$), $\sigma_n^{(s)} \gg \sigma_v$, so the idler capacity (23) is only slightly lower than the signal capacity (19): The idler is a very good copy of the signal. It also follows from the aforementioned results that the total output capacity

$$C_t^{(s)} = \ln[1+\sigma_x^{(s-1/2)}/\sigma_n^{(s-1/2)}]^{1/2}. \quad (24)$$

Equation (24) shows that the total output capacity equals the intermediate signal capacity: Although two-mode amplification redistributes information between the signal and idler, it conserves the total information, as stated in Sec. 2. In the high-loss regime, $C_t^{(s)} - C_1^{(s)} \approx 1/4s \ll 1$, so the idler contains (almost) no extra information. Nonetheless, it is useful to have an extra copy of the signal (for broadcasting or monitoring). Notice that the diagonal entries and determinants of the covariance matrices (21) and (22) depend on ν^2, so the imaginary sideband and total capacities are the same as their real counterparts.

5. One-mode phase-sensitive links

Each stage in a one-mode PS link consists of an attenuator followed by a one-mode PS amplifier, as illustrated in Fig. 5. By combining Eqs. (5) and (8), one finds that the composite IO equation for the first stage is

$$y^{(1)} = (\lambda\tau)y^{(0)} + (\lambda\rho)v^{(1)}, \quad (25)$$

where $y^{(0)}$ and $y^{(1)}$ are the input and output signal quadratures, respectively, and $v^{(1)}$ is the input loss-mode quadrature. For the in-phase (real) quadrature the dilation factor $\lambda = \mu+\nu$, whereas for the out-of-phase (imaginary) quadrature $\lambda = \mu-\nu$.

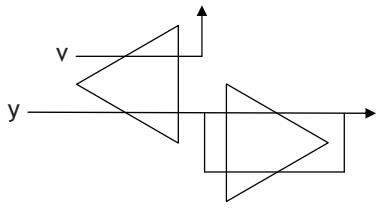

Fig. 5. Architecture of a stage in a one-mode phase-sensitive link. An attenuator ($\triangleleft$) is followed by a one-mode amplifier ($\triangleright$). The closed loop around the amplifier indicates that the signal interacts with itself.

#144953 - $15.00 USD Received 28 Mar 2011; accepted 19 Apr 2011; published 6 Jun 2011

By iterating Eq. (25), one finds that the composite IO equation for an s-stage PS link is

$$y^{(s)} = (\lambda\tau)^s y^{(0)} + (\lambda\rho)\sum_{r=1}^{s}(\lambda\tau)^{s-r}v^{(r)}, \tag{26}$$

where $v^{(r)}$ is the loss-mode (noise) quadrature associated with stage r. Hence, the output signal and noise strengths are

$$\sigma_x^{(s)} = (\lambda\tau)^{2s}\sigma_x^{(0)}, \tag{27}$$

$$\sigma_n^{(s)} = \{(\lambda\tau)^{2s} + (\lambda\rho)^2[1-(\lambda\tau)^{2s}]/[1-(\lambda\tau)^2]\}\sigma_v, \tag{28}$$

respectively. Equations (27) and (28) are consistent with previous results [12, 24]. On the right side of the latter equation, the first term represents transmitted signal fluctuations, whereas the other terms represent accumulated loss-mode fluctuations.

For a balanced link, the in-phase gain compensates loss [$(\mu+\nu)\tau = 1$], so the real signal is conserved. The output strengths

$$\sigma_x^{(s)} = \sigma_x^{(0)}, \tag{29}$$

$$\sigma_n^{(s)} = [1+s(L-1)]\sigma_v. \tag{30}$$

The NF of a one-mode PS link is $1+s(L-1) \approx sL$, which is lower than that of the associated PI link by a factor of 2 (3 dB). It follows from these results and Eq. (1) that the real output capacity

$$C_r^{(s)} \approx \ln[1+\sigma_x^{(0)}/\sigma_v sL]^{1/2}. \tag{31}$$

No noise is added by the one-mode PS amplifiers. The output capacity is lower than the input capacity because of the noise added by the attenuators in the link.

In contrast, even for a balanced link the out-of-phase gain does not compensate loss [$(\mu-\nu)\tau = \tau/(\mu+\nu) = \tau^2$], so the imaginary signal is attenuated. The output strengths

$$\sigma_x^{(s)} = \sigma_x^{(0)}/L^{2s}, \tag{32}$$

$$\sigma_n^{(s)} = 1/L^{2s} + (1-1/L^{2s})/(L+1)$$
$$= (1+1/L^{2s-1})/(L+1). \tag{33}$$

The largest noise contribution (which is of order $1/L$) comes from the last stage in the link. Because the output signal strength is lower than the input strength by a factor of L^{2s}, the NF of the link is $(L^{2s}+L)/(L+1) \approx L^{2s-1}$. Hence, the imaginary output capacity

$$C_i^{(s)} \approx \ln[1+\sigma_x^{(0)}/\sigma_v L^{2s-1}]^{1/2}. \tag{34}$$

Even though the output fluctuations are weaker than the input vacuum fluctuations, the output signal is much weaker than the input signal, so the imaginary output capacity is almost zero: Fiber losses obscure the information in the imaginary quadrature, as stated in Sec. 2. For this reason, a one-mode PS link has a lower capacity than the corresponding two-mode PI link.

6. Two-mode phase-sensitive links

Two-mode PS links are sequences of attenuators followed by two-mode PS amplifiers, as illustrated in Fig. 6. By combining Eqs. (6) and (8), one finds that the (real) IO equations for the first stage are

$$y_1^{(1)} = (\mu\tau)y_1^{(0)} + (\nu\tau)y_2^{(0)} + (\mu\rho)v_k^{(1)} + (\nu\rho)v_l^{(1)}, \tag{35}$$

$$y_2^{(1)} = (\nu\tau)y_1^{(0)} + (\mu\tau)y_2^{(0)} + (\nu\rho)v_k^{(1)} + (\mu\rho)v_l^{(1)}, \tag{36}$$

#144953 - $15.00 USD Received 28 Mar 2011; accepted 19 Apr 2011; published 6 Jun 2011

where y_1 and y_2 are the signal and idler quadratures, respectively, and v_k and v_l are the associated loss-mode quadratures. The other symbols were defined previously.

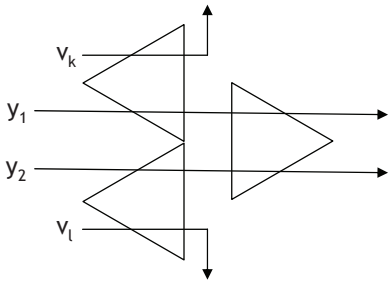

Fig. 6. Architecture of a stage in a two-mode phase-sensitive link. Two attenuators (◁) in parallel are followed by a two-mode amplifier (▷). Modes 1 and 2 are the signal and idler, respectively, and modes k and l are loss modes. Both sidebands are transmitted through the link.

By iterating Eqs. (35) and (36), one obtains the composite IO equations [14]

$$y_1^{(s)} = \tau^s[p_s y_1^{(0)} + q_s y_2^{(0)}] + \rho \sum_{r=1}^{s} \tau^{s-r}[p_{s-r+1} v_k^{(r)} + q_{s-r+1} v_l^{(r)}], \tag{37}$$

$$y_2^{(s)} = \tau^s[q_s y_1^{(0)} + p_s y_2^{(0)}] + \rho \sum_{r=1}^{s} \tau^{s-r}[q_{s-r+1} v_k^{(r)} + p_{s-r+1} v_l^{(r)}], \tag{38}$$

which apply to a two-mode PS link with s stages. The polynomials p_s and q_s are defined by the initial conditions $p_1 = \mu$ and $q_1 = \nu$, together with the recursion relations $p_{r+1} = \mu p_r + \nu q_r$ and $q_{r+1} = \mu q_r + \nu p_r$. By solving these equations, one finds that

$$p_s = [(\mu+\nu)^s + (\mu-\nu)^s]/2, \tag{39}$$

$$q_s = [(\mu+\nu)^s - (\mu-\nu)^s]/2. \tag{40}$$

If the input quadratures are equal and in-phase with the transfer coefficients (positive), the (common) output quadrature $x_j^{(s)} = [(\mu+\nu)\tau]^s x^{(0)}$, so the entries of the output signal covariance matrix

$$\langle x_i x_j \rangle = [(\mu+\nu)\tau]^{2s} \sigma_t/2, \tag{41}$$

where σ_t is the total input strength and the superscript s was omitted for brevity. (In this section, we do not abbreviate $\langle x_i x_j \rangle$ by $\sigma_{x_{ij}}$, to avoid the use of multiple subscripts.) Because most of the noise variables in Eqs. (37) and (38) are independent, the (common) output noise variance and correlation

$$\langle n_j^2 \rangle/\sigma_v = \tau^{2s}(p_s^2 + q_s^2) + \rho^2 \sum_{r=1}^{s} \tau^{2(s-r)}(p_{s-r+1}^2 + q_{s-r+1}^2), \tag{42}$$

$$\langle n_1 n_2 \rangle/\sigma_v = \tau^{2s}(2p_s q_s) + \rho^2 \sum_{r=1}^{s} \tau^{2(s-r)}(2p_{s-r+1} q_{s-r+1}), \tag{43}$$

respectively. (We also do not abbreviate $\langle n_i n_j \rangle$.)

The link is balanced if $(\mu+\nu)\tau = 1$. This condition can be rewritten as $G_0 = L$, where $G_0 = (\mu+\nu)^2$ is the in-phase (power) gain and L is the (power) loss of each stage. By making

#144953 - $15.00 USD Received 28 Mar 2011; accepted 19 Apr 2011; published 6 Jun 2011

these substitutions in Eqs. (42) and (43), and doing the summations, one finds that

$$\langle n_j^2\rangle/\sigma_v = [1+s(L-1)+(1+1/L^{2s-1})/(L+1)]/2, \quad (44)$$

$$\langle n_1 n_2\rangle/\sigma_v = [1+s(L-1)-(1+1/L^{2s-1})/(L+1)]/2. \quad (45)$$

In the high-loss regime, $\langle n_j^2\rangle \approx sL\sigma_v/2 \approx \langle n_1 n_2\rangle$. The output sidebands produced by a two-mode PS link are strongly correlated and the NF of the link ($sL/2$) is lower than that of the associated two-mode PI link by a factor of 4 (6 dB) [14,25]. A difference of 5.5 dB was observed in a recent experiment [26]. For the special case in which $s=1$, $\langle n_j^2\rangle/\sigma_v = (L+1/L)/2$ and $\langle n_1 n_2\rangle/\sigma_v = (L-1/L)/2$, which tend to 1 and 0, respectively, as L tends to 1.

The individual and total information capacities are determined by the covariance matrices

$$K_y = \begin{bmatrix} (\alpha+\beta+\gamma) & (\alpha+\beta-\gamma) \\ (\alpha+\beta-\gamma) & (\alpha+\beta+\gamma) \end{bmatrix}, \; K_n = \begin{bmatrix} (\beta+\gamma) & (\beta-\gamma) \\ (\beta-\gamma) & (\beta+\gamma) \end{bmatrix}, \quad (46)$$

where $\alpha = \sigma_t/2$, $\beta = [1+s(L-1)]\sigma_v/2$ and $\gamma = [(1+L^{2s-1})/(L+1)]\sigma_v/2$. (Notice that $\gamma \ll \beta$.) First, the (common) sideband capacity

$$C_j = \ln[1+\alpha/(\beta+\gamma)]^{1/2}. \quad (47)$$

By calculating the determinants of the covariance matrices, one finds that the total capacity

$$C_t = \ln(1+\alpha/\beta)^{1/2}. \quad (48)$$

[Notice that the largest terms in the determinant (α^2) cancel, so the capacity is determined by smaller terms. This fact requires the variance and correlation calculations to be done accurately.] The sideband capacity is lower than the total capacity (as it must be), but is only slightly lower. (The relative difference is of order $1/L^2$.) This means that most (almost all) of the information is shared between the sidebands. They are nearly perfect copies of each other [14]. The common capacity

$$C \approx \ln(1+\sigma_t/\sigma_v sL)^{1/2}. \quad (49)$$

The (information) SNR $\sigma_t/\sigma_v sL$ is larger than the SNR for the corresponding PI link by a factor of 2 (equal total input powers) or a factor of 4 (equal input sideband powers). These SNR increases are equivalent to capacity increases of 1/2 or 1 bit per quadrature, respectively. The imaginary quadratures transport information in a similar way.

Although the physical-mode calculation is straightforward, the superposition-mode calculation is instructive. Define the sum and difference modes $y_\pm = (y_1 \pm y_2)/2^{1/2}$, respectively. Then, by combining Eqs. (35) and (36), one obtains the superposition-mode IO equations

$$y_\pm^{(1)} = (\lambda_\pm \tau) y_\pm^{(0)} + (\lambda_\pm \rho) v_\pm^{(1)}. \quad (50)$$

Equations (50) are identical to the one-mode equations (11). Hence, the modes propagate independently. The real sum-mode information is transmitted and the difference-mode information is lost. In contrast, the imaginary sum-mode information is lost and the difference-mode information is transmitted. So two quadratures are transported (just like PI links), but with higher efficiencies (NFs lower by a factor of 2). It follows from Eqs. (15) and (17) that, for a balanced link, the output noise strengths

$$\langle n_+^2\rangle/\sigma_v = 1+s(L-1), \quad (51)$$

$$\langle n_-^2\rangle/\sigma_v = (1+1/L^{2n-1})/(L+1). \quad (52)$$

#144953 - $15.00 USD Received 28 Mar 2011; accepted 19 Apr 2011; published 6 Jun 2011

For the special case in which $s = 1$, $\langle n_+^2 \rangle = L$ and $\langle n_-^2 \rangle = 1/L$, both of which tend to 1 as L tends to 1. By using the identities $n_1 = (n_+ + n_-)/2^{1/2}$ and $n_2 = (n_+ - n_-)/2^{1/2}$, one can show that Eqs. (51) and (52) are equivalent to Eqs. (44) and (45).

It can be shown that the capacity is maximized by using uncorrelated superposition-mode inputs [7]. In this case, the covariance matrices

$$K_y = \begin{bmatrix} \alpha_+ + \beta_+ & 0 \\ 0 & \alpha_- + \beta_- \end{bmatrix}, \; K_n = \begin{bmatrix} \beta_+ & 0 \\ 0 & \beta_- \end{bmatrix}, \tag{53}$$

where $\alpha_+ = \sigma_+$, $\alpha_- = \sigma_-/L^{2s}$, $\beta_+ = [1 + s(L-1)]\sigma_v$ and $\beta_- = (1 + L^{2s-1})\sigma_v/(L+1)$. Hence, the individual capacities

$$C_\pm = \ln(1 + \alpha_\pm/\beta_\pm)^{1/2}, \tag{54}$$

and the total capacity $C_t = C_+ + C_-$. If $\alpha_- = 0$ (as assumed previously), $C_- = 0$ and $C_t = \ln(1 + \alpha_+/\beta_+)^{1/2}$, which is consistent with the physical-mode result. However, the superposition-mode calculation is easier and the superposition-mode picture provides more physical insight.

The superposition-mode picture also sheds light on PI links. Such links are inefficient, because they divide the input information equally between the sum and difference modes, and the difference-mode information is promptly lost. If one replaces σ_+ by $\sigma_t/2$ in the sum-mode capacity, one recovers the PI signal capacity (in the high-loss regime). So another explanation of the 3-dB difference between the SNRs associated with PI and PS links is that in the former, half the information is discarded!

The preceding results apply to links with pairs of CS inputs. For links with individual CS inputs, one can use PI amplifiers before the links to generate the idlers (copy the signals). Detailed studies of the noise properties of links with copiers were made in [14, 25]. Just as copiers increase the link NFs slightly (by amounts of order $1 \ll L$), so also do they decrease the link capacities slightly.

7. Summary

In this paper, detailed studies were made of the information capacities of communication links made with one- and two-mode parametric amplifiers. These studies were based on homodyne detection of (complex) amplitude-keyed signals. The input signals were assumed to be coherent states (CS), which have amplitude fluctuations with Gaussian statistics. If such signals (and their associated idlers) propagate through a sequence of (linear) attenuators and amplifiers, their amplitude statistics remain Gaussian. Hence, the output signal–idler pairs are specified completely by their amplitude means, variances and correlations.

The amount of information (capacity) that can be encoded in an input signal depends logarithmically on the input signal-to-noise (SNR) ratio, which is the square of the mean quadrature divided by the quadrature variance. For a CS signal, the quadrature SNR is $4\langle p \rangle$, where $\langle p \rangle$ is the number of photons. For two CS inputs, the capacity depends on how information is distributed between the signal and idler (sidebands). If the total input power is fixed, the capacity associated with two correlated (or anti-correlated) inputs equals that associated with one input, and the capacity associated with two uncorrelated inputs is higher, by a factor of almost 2. However, the use of uncorrelated inputs does not maximize the output information, because of the combined effects of attenuation and amplification on the sidebands.

Parametric amplification is made possible by four-wave mixing (FWM) in fibers. The degenerate FWM process called inverse modulation interaction (MI) always provides one-mode PS amplification. MI and the non-degenerate FWM process called phase conjugation (PC) provide two-mode PI amplification if the input idler is zero, and two-mode PS amplification if the idler is nonzero. (One can generate such an idler using a second transmitter, or by copying the signal

#144953 - $15.00 USD Received 28 Mar 2011; accepted 19 Apr 2011; published 6 Jun 2011

prior to transmission.) Parametric amplification differs from erbium-doped and Raman fiber amplification because it can involve one or two (light) modes and can be PI or PS.

The noise figure (NF) of a communication link is defined as the input SNR divided by the output SNR. The NF of a (balanced) one-mode PS link is approximately sL, where s is the number of stages in the link and L is the loss of each stage. Noise is added by the loss modes of the fibers (attenuators), which have nonzero input fluctuations. The NF of a two-mode PI link is approximately $2sL$. Extra noise is added by the idlers, which also have nonzero input fluctuations. In contrast, the NF of a two-mode PS link is approximately $sL/2$. Once again, noise is added by the attenuators and idlers. However, in the amplifiers the sideband amplitudes add coherently (factor of 4 increase in strength), whereas the sideband fluctuations add incoherently (factor of 2 increase), so PS amplification reduces the link NF by a factor of 4 (6 dB) relative to PI amplification. (An improvement of 5.5 dB was demonstrated experimentally.) Two-mode links also produce output idlers that are excellent copies of the signals.

Amplification and attenuation have significant effects on the information carried by a signal. Amplification stretches the in-phase quadrature and squeezes the out-of-phase quadrature. Neither process decreases the capacity by itself (because the coherent and incoherent components are dilated by the same amount). However, the squeezed information produced by amplification is swamped by the noise associated with subsequent attenuation. Because only stretched information survives, it is best to launch information in whichever quadrature(s) will be stretched during propagation. For one-mode amplification, this quadrature is the in-phase (real) quadrature, whereas for two-mode amplification, they are the real sum-mode and imaginary difference-mode quadratures (which correspond to correlated and anti-correlated inputs of equal strength, respectively).

For balanced links, the input and output signal strengths are equal, and the information capacity is limited by the noise added to the signal during propagation. For a one-mode PS link, the real quadrature is transmitted optimally (with only attenuation noise), whereas the imaginary quadrature is attenuated and the information it carries is lost. This is a serious deficiency of one-mode PS links (unless the signals are differential phase-shift keyed or the links incorporate a phase-diversity scheme). For a two-mode PI link, both quadratures are degraded by noise from the attenuators and amplifiers. However, both quadratures are transmitted (neither is attenuated). Although the NF of this (standard) link is higher than that of the corresponding one-mode link, its ability to transport both quadratures gives it a higher capacity. For a two-mode PS link, the real sum-mode quadrature and the imaginary difference-mode quadrature are transmitted optimally (with only attenuation noise), whereas the other quadratures are attenuated and the information they carry is lost. The NFs of two-mode PS links are 6-dB lower than those of their PI counterparts (if the signal powers are equal), which allows them to transport 1 extra bit per quadrature (2 extra bits per mode). To put this result in perspective, an on-off keyed system with a bit rate of 100-Gb/s and a channel spacing of 50-GHz has a spectral efficiency of 2 b/s-Hz. Two-mode PS amplifiers are compatible with multiple-stage (repeatered) links and are well suited to unrepeatered links (festoons).

The preceding discussion of information capacity does not account for nonlinear effects in the transmission fibers (four-wave mixing, and self- and cross-phase modulation). These processes increase the (complex) amplitude fluctuations of the signals, which decrease their information capacities concomitantly [27–30]. The capacity formulas derived herein are useful upper bounds, whose dependences on the system parameters are evident.

#144953 - $15.00 USD Received 28 Mar 2011; accepted 19 Apr 2011; published 6 Jun 2011

Appendix: Comparison of the quantal and semi-classical results

The coherent state (CS) $|\alpha\rangle$ is defined by the eigenvalue equation

$$a|\alpha\rangle = \alpha|\alpha\rangle, \tag{55}$$

where a is a mode operator, α is a complex parameter and $|\ \rangle$ is a ket vector. The mode operator satisfies the commutation relation (CR) $[a,a^\dagger]=1$, where $[\ ,\ ]$ is a commutator and $\dagger$ is a hermitian conjugate. It follows from Eq. (55) that the expectation value $\langle a\rangle = \alpha$, for which reason α is called the mode amplitude. The quadrature operator

$$q(\theta) = (ae^{-i\theta} + a^\dagger e^{i\theta})/2^{1/2}, \tag{56}$$

where θ is the local-oscillator (LO) phase, and the quadrature-deviation operator $\delta q(\theta) = q(\theta) - \langle q(\theta)\rangle$. By combining Eqs. (55) and (56) with the CR, one finds that the quadrature mean (first-order moment) $\langle q(\theta)\rangle = (\alpha e^{-i\theta} + \alpha^* e^{i\theta})/2^{1/2}$, which depends on both the mode amplitude and LO phase, and the quadrature variance (second-order moment) $\langle \delta q^2\rangle = 1/2$, which does not depend on the amplitude or phase.

Multiple-mode parametric processes are governed by the input-output (IO) equations

$$b_j = \sum_k (\mu_{jk} a_k + \nu_{jk} a_k^\dagger), \tag{57}$$

where a_j is an input-mode operator, b_j is an output-mode operator, and μ_{jk} and ν_{jk} are transfer coefficients. The input modes satisfy the CRs $[a_j,a_k]=0$ and $[a_j,a_k^\dagger]=\delta_{jk}$, where δ_{jk} is the Kronecker delta function. The output modes satisfy similar CRs, which imply that

$$\sum_l (\mu_{jl}\nu_{kl} - \mu_{kl}\nu_{jl}) = 0, \tag{58}$$

$$\sum_l (\mu_{jl}\mu_{kl}^* - \nu_{jl}\nu_{kl}^*) = \delta_{jk}. \tag{59}$$

Suppose that the inputs are CS with amplitudes α_j. [If some $\alpha_j = 0$, those inputs are vacuum states (VS).] Then the output amplitudes (first-order moments) $\beta_j = \sum_k (\mu_{jk}\alpha_j + \nu_{jk}\alpha_k^*)$. There are two standard ways to calculate the higher-order output moments. In the first method, one combines Eqs. (57) and calculates expectation values using the properties of CS [Eq. (55) and its hermitian conjugate] and the CRs. In the second method, one rewrites the operators as

$$a_j = \alpha_j + v_j, \quad b_j = \beta_j + w_j, \tag{60}$$

where the auxiliary (noise) operators v_j and w_j also satisfy the CRs and Eqs. (57), and calculates expectation values using the properties of VS ($v_j|0\rangle = 0$). The second method will be used herein (because it is similar to the semi-classical method, which will be described shortly).

The output quadrature and quadrature-deviation operators are also defined by Eq. (56), with a replaced by b_j and w_j, respectively. It follows from these definitions and Eqs. (57) that the output quadratures $\langle q_j(\theta_j)\rangle = (\beta_j e^{-i\theta_j} + \beta_j^* e^{i\theta_j})/2^{1/2}$ and the output-quadrature correlations

$$\langle \delta q_i(\theta_i)\delta q_j(\theta_j)\rangle = \langle (w_i e^{-i\theta_i} + w_i^\dagger e^{i\theta_i})(w_j e^{-i\theta_j} + w_j^\dagger e^{i\theta_j})\rangle/2. \tag{61}$$

By combining Eqs. (61) with the noise moments

$$\begin{aligned} \langle w_i w_j\rangle &= \sum_k \mu_{ik}\nu_{jk}, \quad \langle w_i w_j^\dagger\rangle = \sum_k \mu_{ik}\mu_{jk}^*, \\ \langle w_i^\dagger w_j\rangle &= \sum_k \nu_{ik}^*\nu_{jk}, \quad \langle w_i^\dagger w_j^\dagger\rangle = \sum_k \nu_{ik}^*\mu_{jk}^*, \end{aligned} \tag{62}$$

one finds that the quadrature correlations

$$\langle \delta q_i(\theta_i)\delta q_j(\theta_j)\rangle = \sum_k (\mu_{ik}e^{-i\theta_i} + \nu_{ik}^* e^{i\theta_i})(\mu_{jk}^* e^{i\theta_j} + \nu_{jk} e^{-i\theta_j})/2. \tag{63}$$

#144953 - $15.00 USD Received 28 Mar 2011; accepted 19 Apr 2011; published 6 Jun 2011

When $i = j$, the right side of Eq. (63) is manifestly real. When $i \neq j$, the right side of Eq. (63) involves summations of $\mu_{ik}\mu^*_{jk}e^{i(\theta_j-\theta_i)}$, $\mu_{ik}\nu_{jk}e^{-i(\theta_i+\theta_j)}$, $\nu^*_{ik}\mu^*_{jk}e^{i(\theta_i+\theta_j)}$ and $\nu^*_{ik}\nu_{jk}e^{i(\theta_i-\theta_j)}$. Equation (58) implies that the sum of the second and third terms is real, whereas Eq. (59) implies that the sum of the first and fourth terms is real. Hence, the quadrature-correlation formula predicts real correlations (as it must do).

In the semi-classical method, one adds to each complex amplitude α_j a complex random variable v_j. (Although the same notation is used for quantal operators and classical random variables, the meaning should be clear from the context.) The random variables have Gaussian statistics, and the moments $\langle v_j\rangle = 0$, $\langle v_j v_k\rangle = 0$ and $\langle v_j v^*_k\rangle = \delta_{jk}/2$. For each input, the quadrature mean $\langle \alpha_j + v_j\rangle = \alpha_j$ and the quadrature variance $\langle v^2 e^{-i2\theta} + 2|v|^2 + (v^*)^2 e^{i2\theta}\rangle/2 = 1/2$, which are exactly the results associated with a CS, and the number mean $\langle|\alpha_j + v_j|^2\rangle = |\alpha_j|^2 + 1/2$, which is approximately the result associated with a CS. Hence, one describes the semi-classical method by saying that 1/2 noise photon is added to each mode. In the semi-classical method, the amplitudes and random variables obey the same IO equations as their quantal counterparts [Eqs. (57) with † replaced by $*$], so the method produces the same quadrature-correlation formula [Eq. (61)]. It follows from Eqs. (57) and the stated input moments that the output moments

$$\begin{aligned} \langle w_i w_j\rangle &= \textstyle\sum_k \mu_{ik}\nu_{jk}, & \langle w_i w^\dagger_j\rangle &= \textstyle\sum_k \mu_{ik}\mu^*_{jk} - \delta_{ij}/2, \\ \langle w^\dagger_i w_j\rangle &= \textstyle\sum_k \nu^*_{ik}\nu_{jk} + \delta_{ij}/2, & \langle w^\dagger_i w^\dagger_j\rangle &= \textstyle\sum_k \nu^*_{ik}\mu^*_{jk}. \end{aligned} \tag{64}$$

By comparing Eqs. (62) and (64), one finds that the semi-classical model predicts correctly all of the random-variable moments required to evaluate the quadrature correlations ($i \neq j$). It underestimates the moment $\langle w_i w^\dagger_i\rangle$ by 1/2 and overestimates $\langle w^\dagger_i w_i\rangle$ by the same amount. However, the only quadrature moments that depend on these quantities are the variances $\langle \delta q_i(\theta_i)^2\rangle$, which depend on their sums and, hence, are also correct. In summary, the semi-classical method, which consists of adding Gaussian amplitude fluctuations with variance 1/2 to each classical amplitude, reproduces exactly the quadrature means and variances of CS inputs, and the output quadrature means, variances and correlations produced by sequences of parametric processes.

Acknowledgment

We acknowledge a useful discussion with E. Agrell.

#144953 - $15.00 USD Received 28 Mar 2011; accepted 19 Apr 2011; published 6 Jun 2011